Overview of the LIBRA Light Ion Beam Fusion Conceptual Design

G.A. Moses, G.L. Kulcinski, D. Bruggink, R.L. Engelstad, E.G. Lovell, J.J. MacFarlane, Z. Musicki, R.R. Peterson, M.E. Sawan, I.N. Sviatoslavsky, L.J. Wittenberg, G. Kessler, U. von Möllendorff, E. Stein, D. Cook, R. Olson, I. Smith, P. Corcoran, H. Nishimoto, J. Fockler

October 1988

UWFDM-781

Presented at the 8th Topical Meeting on the Technology of Fusion Energy, 9–13 October 1988, Salt Lake City UT.

FUSION TECHNOLOGY INSTITUTE

UNIVERSITY OF WISCONSIN

MADISON WISCONSIN

Overview of the LIBRA Light Ion Beam Fusion Conceptual Design

G.A. Moses, G.L. Kulcinski, D. Bruggink, R.L. Engelstad, E.G. Lovell, J.J. MacFarlane, Z. Musicki, R.R. Peterson, M.E. Sawan, I.N. Sviatoslavsky, L.J. Wittenberg, G. Kessler, U. von Möllendorff, E. Stein, D. Cook, R. Olson, I. Smith, P. Corcoran, H. Nishimoto, J. Fockler

Fusion Technology Institute
University of Wisconsin
1500 Engineering Drive
Madison, WI 53706

http://fti.neep.wisc.edu

October 1988

UWFDM-781

Presented at the 8th Topical Meeting on the Technology of Fusion Energy, 9–13 October 1988, Salt Lake City UT.

OVERVIEW OF THE LIBRA LIGHT ION BEAM FUSION CONCEPTUAL DESIGN

G.A. Moses, G.L. Kulcinski, D. Bruggink, R. Engelstad, E. Lovell, J. MacFarlane,
Z. Musicki, R. Peterson, M. Sawan, I. Sviatoslavsky, L. Wittenberg
University of Wisconsin Fusion Technology Institute and Fusion Power Associates
1500 Johnson Drive, Madison, WI 53706-1687 (608) 263-3368

G. Kessler, U. von Möllendorff, E. Stein
Institut für Neutronen Physik und Reaktortechnik, Kernforschungszentrum
D-7500 Karlsruhe, Postfach 3640, West Germany 011-49-7247-822440 x441

D. Cook and R. Olson
Sandia National Laboratory, Division 1251
Albuquerque, NM 87185 (505) 844-5429

I. Smith, P. Corcoran, H. Nishimoto, J. Fockler
Pulse Sciences, Inc.
600 McCormick Street, San Leandro, CA 94577 (415) 632-5100

ABSTRACT

The LIBRA light ion beam fusion commercial reactor study is a self-consistent conceptual design of a 330 MWe power plant with an accompanying economic analysis. Fusion targets are imploded by 4 MJ shaped pulses of 30 MeV Li ions at a rate of 3 Hz. The target gain is 80, leading to a yield of 320 MJ. The high intensity part of the ion pulse is delivered by 16 diodes through 16 separate z-pinch plasma channels formed in 100 torr of helium with trace amounts of lithium. The blanket is an array of porous flexible silicon carbide tubes with $Li_{17}Pb_{83}$ flowing downward through them. These tubes (INPORT units) shield the target chamber wall from both neutron damage and the shock overpressure of the target explosion. The target chamber is "self-pumped" by the target explosion generated overpressure into a surge tank partially filled with $Li_{17}Pb_{83}$ that surrounds the target chamber. This scheme refreshes the chamber at the desired 3 Hz frequency without excessive pumping demands. The blanket multiplication is 1.2 and the tritium breeding ratio is 1.4. The direct capital cost of LIBRA is estimated to be $2200/kWe.

INTRODUCTION

The LIBRA study is a self-consistent conceptual design of a light ion driven commercial fusion power reactor.[1] Other LIB reactor designs include UTLIF,[2] ADLIB,[3] and EAGLE.[4] A point design for LIBRA was completed and a cost estimate was based upon it. A cost scaling was then done to study the effect of redesigning to different power levels. Specific design parameters are given in Table I. A schematic of the design is given in Fig. 1 and a cross section of the reactor chamber is shown in Fig. 2.

In this paper, the emphasis will be upon the target performance, driver design, diode concept, ion beam transport, and the target driven blast wave. A companion paper in these proceedings[5] will include the target chamber design and response to the micro-explosion, the neutronics and energy recovery, and tritium fueling, breeding, and inventory. The economic aspects of LIBRA will be included and compared to other inertial fusion reactor designs in another paper in these proceedings.[6]

TARGET PERFORMANCE

The target for LIBRA is a generic single shell design similar to that used in the HIBALL study.[7] The initial target configuration is shown in Fig. 3. The configuration at the instant of ignition is also shown. No implosion calculations were done for this specific design, but calculations done for similar targets[8] give us confidence that the energetics of our design (i.e., input energy per unit mass accelerated) is roughly correct. While other designs, unavailable to us for this study, may in fact be required to reach ignition conditions, we feel that this generic design adequately serves our purposes.

The target gain was chosen to be 80 for 4 MJ of ion input energy. This is consistent with published gain estimates[9] as shown in Fig. 4. The power on target of 400 TW is also consistent with published requirements[9] (Fig. 5).

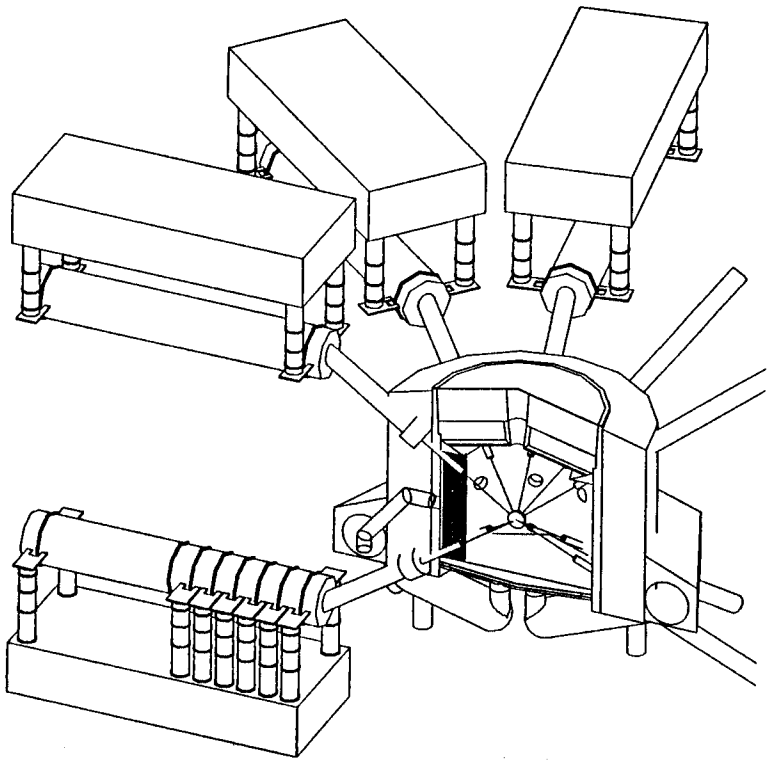

Fig. 1. LIBRA reactor design.

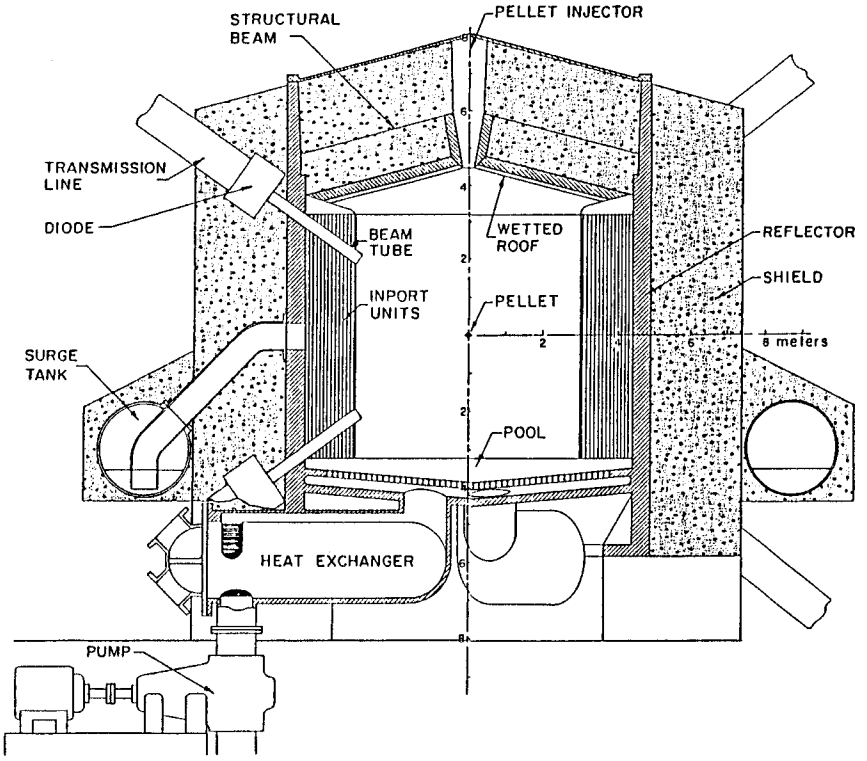

Fig. 2. Cross section of target chamber.

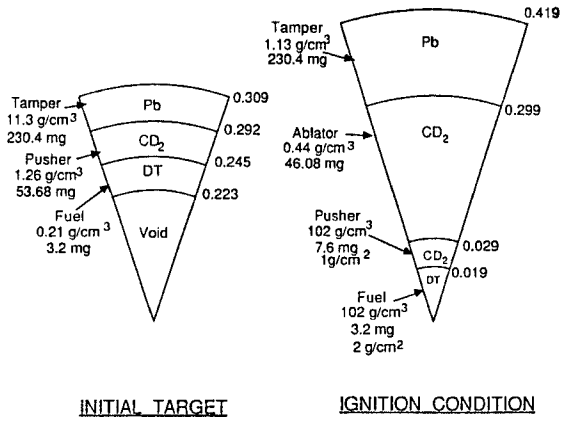

Fig. 3. Generic single shell target design for LIBRA analysis.

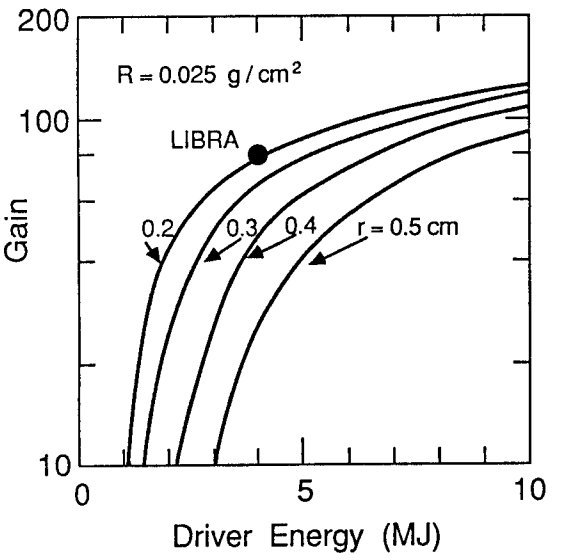

Fig. 4. Comparison of LIBRA gain to LLNL gain estimates [R. Bangerter, Fusion Tech. 13, 348 (1988)].

Coupled thermonuclear burn-radiation hydrodynamic simulations predict that a fuel mass compressed to a ρR-value of 2 g/cm^2 and surrounded by a low-Z pusher with a ρR-value of 1 g/cm^2 burns with a 30% burn-up fraction. For 3.2 mg of DT fuel this results in a thermonuclear yield of 320 MJ.

The x-ray spectrum used for the cavity response calculations is given in Fig. 6. The ion spectrum was assumed to be 2.4 keV DT, 3.8 keV He, 6.6 keV Li, and 198 keV Pb. The x-ray spectrum has both a hard and soft component. The hard part is due to bremsstrahlung x-rays generated by the burning DT escaping through the high-Z tamper material. The soft part is due to radiation from the target once its temperature equilibrates during the expansion phase following burn. The neutron spectrum and subsequent nuclear analysis is given in ref. 5 and will not be included in this paper.

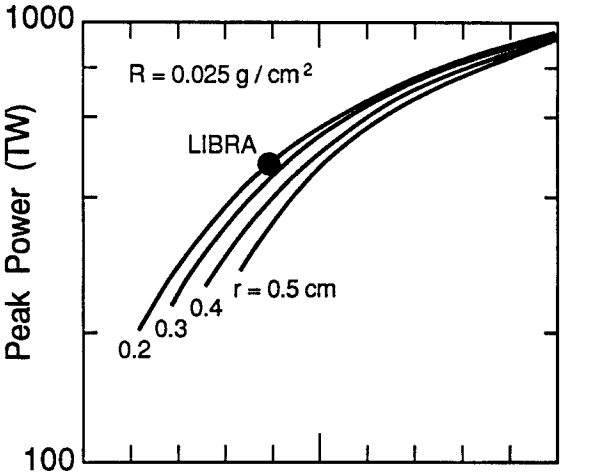

Fig. 5. Comparison of LIBRA power on target to LLNL estimates [R. Bangerter, Fusion Tech. 13, 48 (1988)].

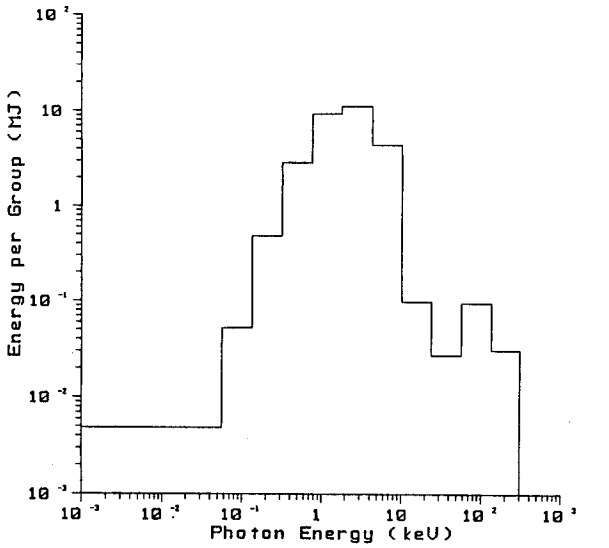

Fig. 6. X-ray spectrum from LIBRA target.

DRIVER DESIGN

The 30 MV pulse generator design for LIBRA[10] (Fig. 1) is like that of Helia[11] and Hermes-III.[12] Pulses of about 1 MV are generated by water dielectric pulseforming lines (PFLs) and delivered through induction cells to a coaxial magnetically insulated vacuum voltage adder (MIVA) that drives the ion diode (Fig. 7).

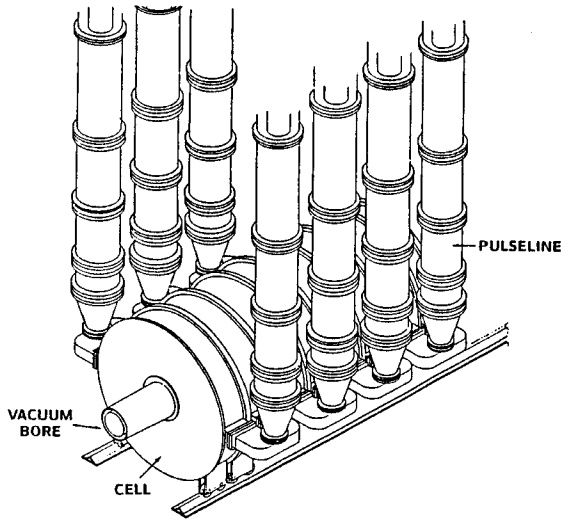

Fig. 7. Pulse line and cell layout.

Hermes-III demonstrates in single-shot mode the technology of the 30 MV LIBRA driver except that the polarity of the voltage adder must be changed to provide a positive output. This and the requirement for a repetitive ion diode are the main technical advances required for the LIBRA driver. The repetitive operation should be achievable by replacing the water dielectric switches used in Helia and Hermes-III by magnetic (saturable reactor) switches like those developed at Lawrence Livermore National Laboratory.[13]

The Helia approach was chosen for LIBRA because it is relatively well demonstrated and well suited to the requirement for many modules. Its use of PFLs in series makes the relatively high impedance needed for each module compatible with the impedance of PFLs of high energy density water dielectric. Also, the series construction of the induction cells and voltage adder allows a low total inductance for the power flow into the vacuum, and hence fast rise-time and accurate pulse shaping.

Beam transport considerations favor the use of a large number of driver modules, while economy of driver design favors the use of fewer modules. A compromise was made at 16 modules. The diode impedance (assumed constant) is 78 Ω; the diode current at 30 MV is 385 kA, the power is 11.5 TW, and with 40 ns diode pulse duration, the diode energy per module is 0.46 MJ. An efficiency of 50% is assumed between diode and target, so that the energy delivered to the target by 16 modules is 3.6 MJ. A shaped pulse with a total of 4 MJ is provided by an additional two pulsed power modules that generate the long "prepulse" before the 3.6 MJ high power part.

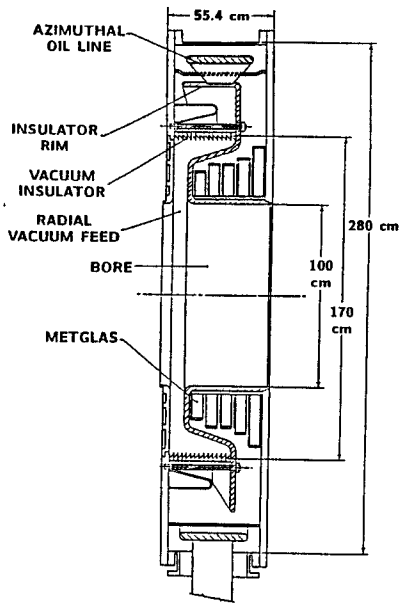

Fig. 8. Side view of 1.15 MV cell.

The induction cell voltage is chosen at 1.15 MV, because the vacuum insulator then just fits within the cell length required for an oil transmission line sized to distribute the 385 kA around the cell. Twenty-six cells are needed in series. The cross section of a single cell is shown in Fig. 8.

The ratio of cell voltage to cell current, 3 Ω, is a convenient impedance for a coaxial water dielectric PFL (shown in Fig. 9). Therefore, the module is driven by 26 PFLs, one per cell. To help achieve a uniform current flow into the vacuum bore, each cell is driven from two sides, Fig. 2; one opposite pair of PFLs drives two adjacent cells in parallel.

The voltage waveform produced by a circuit model of one PFL and cell is shown in Fig. 10. The useful part of the pulse is the 48 ns during which the voltage ramps from just over 1 MV to 1.35 MV, giving the desired average value of 1.15 MV and the desired ramp factor. This waveform was used as input for the voltage adder design.

Voltage waveforms calculated at various places in the PFL and the cell were used to assess the electric stress levels in the PFL and cell and to confirm the volt-second integral on the PFL output switch at saturation and on the cell cores, which it was shown would not saturate until well after the useful pulse is over and the voltage is relatively low.

Stress levels for one module are about 50% of breakdown, and thus reasonably low, though it

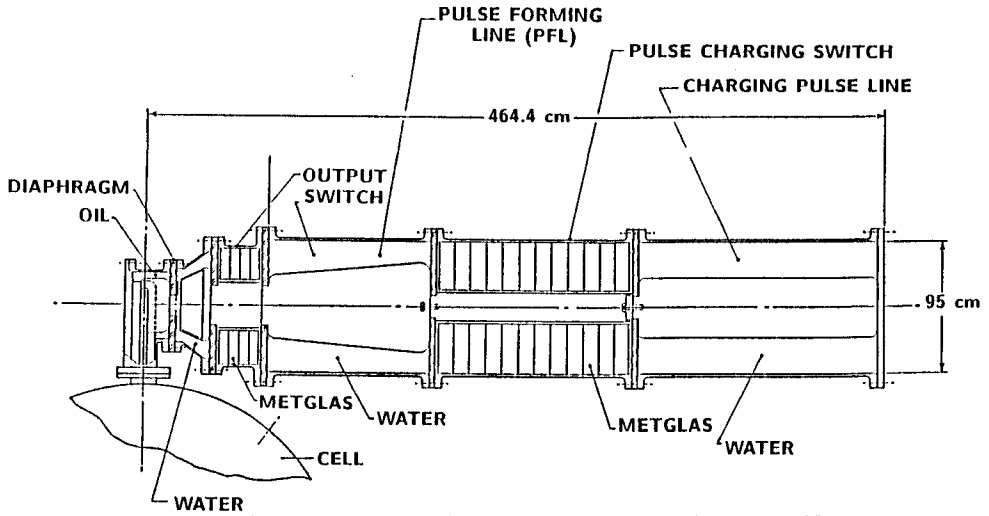

Fig. 9. Water pulse line and connection to cell.

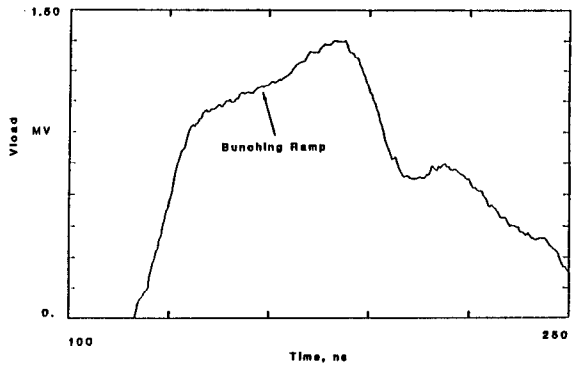

Fig. 10. Pulse injected into voltage adder.

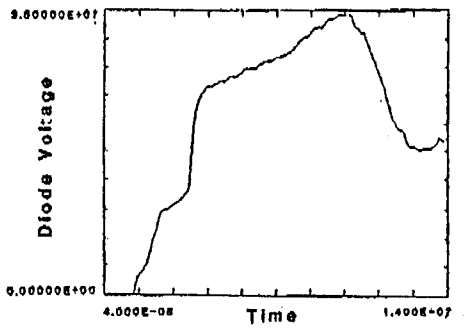

Fig. 11. Diode voltage waveform.

is not known if the reliability would be adequate in continuous operation.

The vacuum interface is at about 60% of breakdown according to J.C. Martin's criterion.[14] It is estimated that this would give very high reliability because the occasional flashover of one insulator section would have a very low probability of causing flashover of any other section.

Stresses in the Metglas cores of the cells are very low (10-15 kV/cm). Stresses in the pulse line switch insulation (250 kV/cm) are larger than those used in existing repetitive switches, but lower than stresses in capacitors.

The magnetically insulated voltage adder (MIVA) was assumed to behave similarly to the MIVA in Hermes-III, though it may be hard to achieve this performance with a positive inner conductor. The MIVA was modelled as 26 transmission line sections in which electron loss was represented by the Sandia R-LOSS model, driven in series by 3 Ω voltage sources with the waveform shown in Fig. 10. It was found that losses on the top of the pulse were small if the wave impedance of each MIVA section was chosen so that the load current was 1.2 times the minimum parapotential current at the voltage in that section. The resulting waveform into the 78 Ω diode is shown in Fig. 11. After the pulse erosion by electron losses, which are assumed to turn on at a field of 150 kV/cm, about 44 ns of useful pulse remain, and 500 kJ are delivered during a voltage ramp from 26 MV to 35 MV.

Figure 2 shows the power pulse of the ion beams after 6.5 m of transport. The ions are assumed to propagate in straight lines, and always to make up 50% of the diode power. For the MIVA driven diode, the pulse is about 5 ns wide; about 4 ns is required to deliver the 225 kJ needed.

ION DIODE

The ion diodes for LIBRA must be very different from those used in experiments today. They must be rep-rateable (10^8 shots/year) and with an extraction geometry. The LIBRA diode concept is a uniform magnetic insulation extraction applied-B diode in coaxial geometry.[15] The anode is annular and the liquid lithium source is in a fritted stainless steel substrate. The

Table I. LIBRA Parameters

General	
Net electric power	331 MW
Gross electric power	441 MW
Thermal power	1160 MW
Recirc. power fraction	0.25
Driver efficiency	0.23
Target gain	80
Fusion gain	18.4
Direct capital cost	$2200/kW
Target Performance	
DT mass	3.2 mg
Input energy	4 MJ
DT yield	320 MJ
Ion yield	28 MJ
X-ray yield	67 MJ
Neutron and gamma yield	218 MJ
Endoergic loss	7 MJ
Neutron multiplication	1.02
Applied-B Diode	
Anode source	Liquid Li
Anode current density	5 kA/cm^2
Anode radius	8.4 cm
Focal length	70 cm
Microdivergence	5 mrad
Macrodivergence	120 mrad
Conversion efficiency	0.80
Helia Pulsed Power	
Waterline energy	11.1 MJ
No. of cells/module	26
Voltage/cell	1.15 MV
Cell diameter	2.9 m
Module diameter	5.15 m
Module length	14.4 m
PFL output voltage	1.15 MV
Impedance	3 Ω
Dielectric	water
Switch type	Metglas saturable reactor

Lithium Ion Beams	
Energy	25-35 MeV
Number high power	16
low power	2
Peak power on target	400 TW
Pulse compression ratio	5
Pulse length on target	9 ns
Current/channel	0.3 MA
Entering on target	1.1 MA
Ion energy transport eff.	0.63
Laser-Guided, Free Standing Channels	
Length	5.4 m
Radius	0.5 cm
Peak B-field	27 kG
Peak current	100 kA
Rise time	1 μs
Voltage drop	1 MV
Cavity	
Gas pressure	100 torr He
Radius to first surface	3 m
Pumping time	300 ms
Impulse on INPORTs	150 Pa-s
Vaporized LiPb mass	9 kg
INPORT Tube Blanket	
Tube material	SiC
Packing fraction	0.33
Coolant/breeder	$Li_{17}Pb_{83}$
Li-6 enrichment	90%
Thickness	1.35 m
Energy multiplication	1.2
Tritium breeding ratio	1.5
Peak end-of-life in chamber wall	200 dpa
Tritium	
Inventory target prep.	696 g
breeder	187 g
Effluent	10 Ci/day

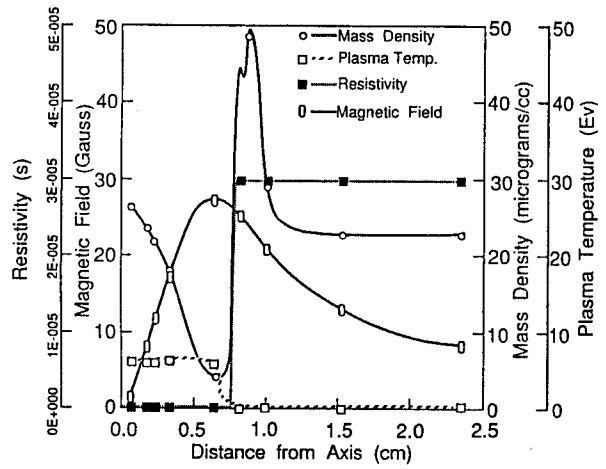

Fig. 12. Plasma channel conditions for ion transport.

anode plasma is formed using the electrohydrodynamic (EHD) effect. A rarefied lithium plasma is injected into the AK gap for electron filling. There is a flux excluder at the cathode tips for impedance control. The channel magnetic field strength is tuned to allow canonical momentum separation of other species than the Li^+ that we want to accelerate. The parameters for the ion diodes are given in Table I.

CHANNEL FORMATION AND BEAM TRANSPORT

The ion beams must be transported from the ion diodes to the target in plasma channels. The channels enter the target chamber in two cones, 35° above and below the horizontal plane containing the target. For each channel, there is a 4.5 meter channel to return the discharge current that leaves the target chamber through the top. The channel parameters are listed in Table I.

The discharge current must be confined to a small region near the axis of the channel. This means that the resistivity must be high away from the channel and low on the axis. Since resistivity decreases rapidly with increasing temperature, this means that the radial temperature profile in the channels must be peaked along the channel axis and low in the region just outside the channel. A small diameter preionizing laser beam and a fast rising discharge current should be advantageous for this channel formation.

A two stage discharge current history where a large main pulse follows a smaller prepulse was first proposed several years ago[16] and this was parameterized by a delay time Δt. Simulations of channel formation in helium gas at a mass density of 2.37×10^{-5} g/cm^3 were performed using the ZPINCH radiation magneto-hydrodynamics computer code.[17] A 1 μs delay time in the discharge current and a laser beam half-width of 2 mm was used. For these values the simulations predict that the magnetic field at 0.5 cm from the channel axis reaches 27 kG and that the average mass density in the channel is approximately 5×10^{-6} g/cm^3 (Fig. 12). These results are acceptable for LIBRA.

BEAM TRANSPORT

The efficiency of individual ion transport from diode to target is determined by two mechanisms. First, the ions must enter the channel within an angular and radial constraint.[18] Ions that have larger angles of incidence and are at relatively large distances from the channel axis are either not trapped by the channel's magnetic field and pass through the background gas never turning back toward the channel axis, or are turned back by the magnetic field but at a large enough radius that they have a small chance of striking the target. Second, the ions must enter the overlap region near the target within an angular constraint that will allow them to hit the target while travelling on a ballistic path.

These two mechanisms were studied by following the trajectories of a random selection of ions in initial angle and radial position as they propagate down the channel using the ION computer code.[19] The magnetic field is assumed to be only in the azimuthal direction and rises linearly from zero on the channel axis to 27 kG at 0.5 cm and falls as 1/r beyond 0.5 cm in the main part of the channel. Within the overlap region, the azimuthal fields fall linearly to zero over an axial distance of 1 cm from the entrance to the region. The ions enter the channels with radial positions distributed in a Gaussian with a half-width of 0.35 cm and with angles of incidence distributed uniformly out to 0.12 radians. In LIBRA there are 18 channels with 9 in each of 2 cones. The channels are 0.5 cm in radius and the target is 0.5 cm in radius, so the distance between the point where the channels begin to overlap and the target surface is 0.43 cm. Calculations predict that about 80% of the ions reach the target.

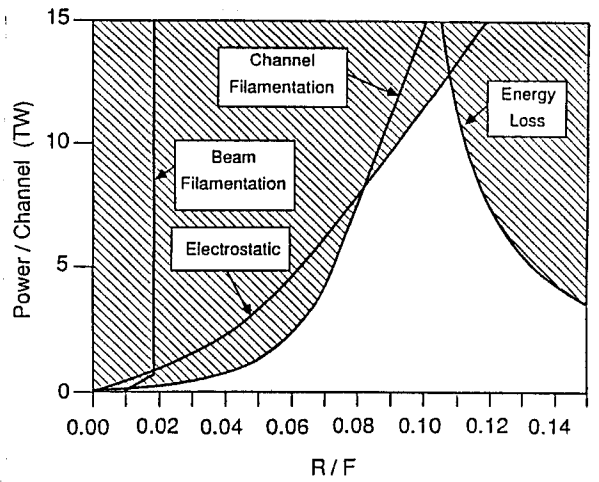

Fig. 13. Propagation "window" for LIBRA ion beams.

Each of the plasma channels in LIBRA must carry several hundred kiloamperes of beam ion current, which can perturb the channels and possibly inhibit the transport of the beam ions. The limits on the ion beam power imposed by the onset of electrostatic instabilities, filamentation of the ion beam and the plasma channel, and beam ion energy loss have been analyzed. The expansion of the channels due to the ion beam has also been analyzed, and does not pose an important constraint. The analysis has followed the formalism developed a number of years ago at the Naval Research Laboratoryy[20] and involves the use of the WINDOW computer code.[21]

The results are shown for LIBRA parameters in Fig. 13. One sees that the input ion beam power per channel is limited to 9 TW at a diode R/F of 0.12, the LIBRA value.

CHANNEL INSULATION

The long channels in LIBRA (or any light ion beam reactor) have a large inductance. Thus, the microsecond rise-time of the current necessary for channel formation requires very large discharge voltages. The potential drop between the channel and the target chamber structure (assumed to be at ground) is 500 kV for LIBRA. To prevent breakdown between the channel and the chamber wall would require a prohibitively large gap. Thus the channel is surrounded by solenoids between the diode structure and the inside row of INPORT units. An axial magnetic field of 32 kG is expected to slow the flow of electrons in the breakdown to a time scale greater than the 1 μs channel

formation time.[22] This allows the diameter of the penetrations for the channels and beams to be 20 cm.

CAVITY ANALYSIS

The response of the He gas and liquid LiPb coating on the INPORT tubes to a LIBRA target explosion was studied using a 1-D radiation-hydrodynamics code, CONRAD.[23] CONRAD calculates the target x-ray and debris ion energy deposition in a background gas and surrounding first surface material using time-dependent point source models. Conservation of mass, momentum, and energy equations are solved in Lagrangian form in a spherical coordinate system. Because CONRAD is a one-dimensional code and the INPORT tubes basically pose a cylindrical boundary, the LiPb first surface is modeled by a thin spherical region at a radius of 3 meters; i.e., the minimum distance from the target to the INPORT tubes.

Target energy absorbed by the background gas is transported throughout the cavity by fluid motion, radiation, and electron thermal conduction. We use a multigroup flux-limited diffusion model to transport radiation. Equations of state and frequency-dependent radiative properties of the chamber gases are tabulated prior to the simulation using a collisional-radiative equilibrium computer code -- IONMIX.[24] IONMIX calculates steady-state ionization populations by balancing collisional ionization rates with the sum of collisional, radiative, and dielectronic recombination rates. The extinction coefficients and emissivities include contributions from bound-bound, bound-free, and free-free transitions, as well as electron scattering.

In addition, CONRAD simulates the vaporization, hydrodynamic motion, and recondensation of the LiPb. Ablation due to the target x-rays is calculated using a volumetric energy deposition model. Energy, reradiated by the cavity gas and the debris ions kinetic energy is assumed to be deposited at the vapor/first surface interface because of their relatively short mean free paths. Heat transfer through the first surface material is computed by solving a 1-D thermal conduction equation. A detailed description of the CONRAD vaporization/condensation model is presented elsewhere in these proceedings.[25]

A schematic representation of the physical processes occurring in the LIBRA target chamber is shown in Fig. 14 After the target explodes, x-ray and debris ion energy is absorbed by the background gas, creating a high-temperature (~ several eV) microfireball at the center of the chamber. The resulting high pressures cause the gas to expand rapidly outward and form a strong shock front ahead of the microfireball. Some of the target x-rays penetrate through the

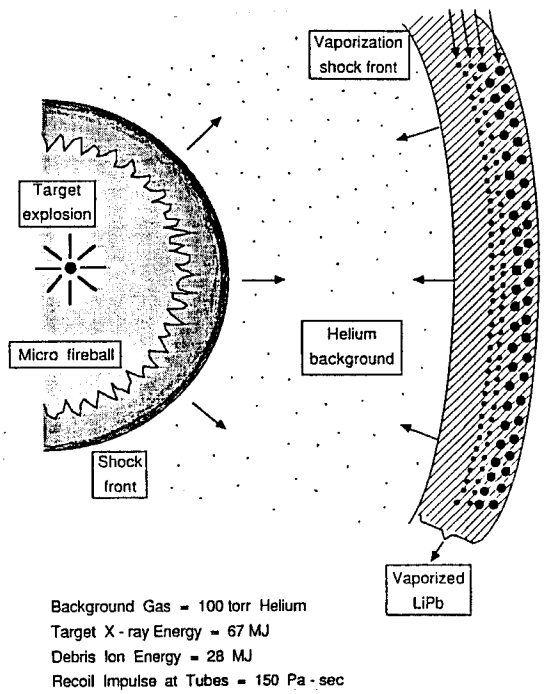

Fig. 14. Schematic of physical processes in target chamber following micro-explosion.

He gas and deposit their energy in a thin layer (~ several microns) of LiPb at the INPORT tubes. Some LiPb is immediately vaporized and, due to the high pressures in the vapor, is hydrodynamically accelerated toward the center of the chamber.

The LIBRA target performance and cavity parameters are listed in Table I. The He gas absorbs approximately 20% of the target x-ray energy and all of the debris ion energy. The remaining 80% of the x-ray energy is absorbed in the LiPb, and immediately vaporizes about 7 kg. The LiPb mass vaporized from the INPORT tubes is shown in Fig. 15 as a function of time. The LiPb vaporization front moves away from the tubes and collides with the outward moving shock front at about 0.1 ms. The high pressures in the LiPb vapor produce a recoil impulse of 150 Pa-s on the tubes. The shock originating from the high-temperature microfireball contributes little to the total impulse on the tubes because it is overwhelmed by the inward moving vaporization front.

Between 10^{-6} and 10^{-4} seconds, an additional 2 kg of LiPb is vaporized as energy radiated by the He gas and LiPb vapor is absorbed at the tubes. Figure 6 shows the radiative flux (solid curve) and radiative energy deposited (dashed curve) at the INPORT tubes as a function of time. The vapor/liquid interface absorbs roughly 4 MJ (i.e., 4 J/cm^2)

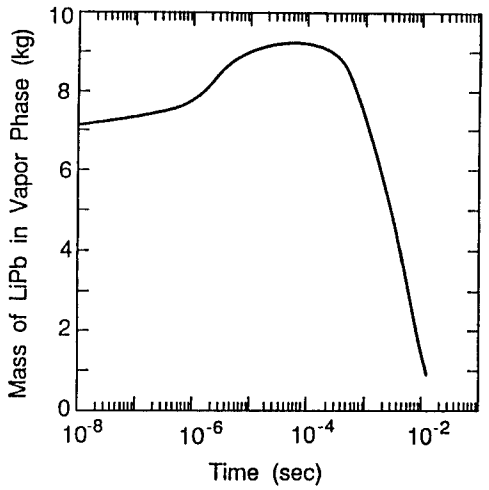

Fig. 15. Lithium-lead mass vaporized vs. time.

by 100 μs. When the radiative energy flux into the liquid exceeds the conductive energy flux through the liquid, the temperature at the surface rises. This produces an increase in the equilibrium (saturation) vapor pressure, and hence the vaporization flux.

At times $\gtrsim$ 1 ms, the LiPb recondenses back onto the tubes. By 10 ms, only 0.8 kg of LiPb remains in the vapor phase, corresponding to a LiPb/He number ratio of 0.007. According to these calculations, the LiPb condensation time would not be expected to limit the shot rate. However, the effects of the noncondensable He gas on the condensation rate have not been considered in our calculations. Preliminary calculations[25] indicate that the He may dramatically slow the LiPb condensation rates. Because of the uncertainties associated with the condensation times, a pumping system has been devised to evacuate the post shot gases from the target chamber.[5]

SUMMARY

The LIBRA conceptual design indicates that light ion beam driven fusion is an excellent candidate for small economical power plants. Technical uncertainties associated with diode design and ion transport to the target remain the major issues associated with light ion fusion. These are of course in addition to target performance and manufacturing that are generic ICF issues.

ACKNOWLEDGEMENTS

This work was supported by Kernforschungszentrum Karlsruhe and Sandia National Laboratory. Computer time was supported by the National Science Foundation through the San Diego Supercomputer Center.

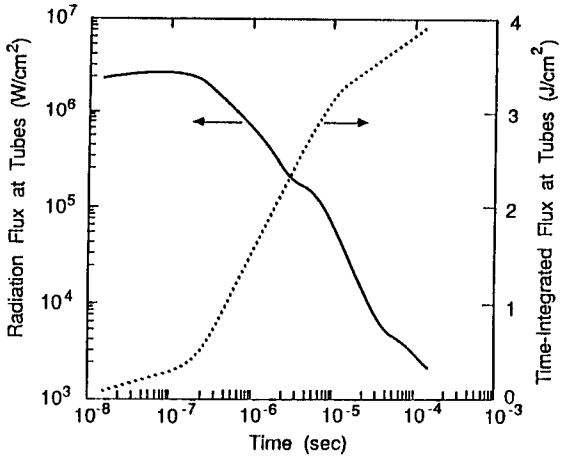

Fig. 16. Radiative flux and deposited energy vs. time.

REFERENCES

1. G.A. MOSES, et al., "LIBRA - A Light Ion Beam Fusion Reactor Conceptual Design," Proceedings of the Beams '88 Conference, July 1988, Karlsruhe, FRG. Also to be published in Lasers and Particle Beams.

2. "Preliminary Design of Light Ion Beam Fusion Reactors, UTLIF (1) & ADLIB-1," University of Tokyo Nuclear Engineering Research Laboratory UTNL-R-0135 (1982).

3. K. NIU and S. KAWATA, "Proposal of Power Plant by Light Ion Beam Fusion," Fusion Technology, 11, 365 (1987).

4. "Light Ion System Analysis and Design-Phase I: Engineering Test Reactor Goal Specification," Research Project 1527, Electric Power Research Institute (April 1982), no author.

5. M. SAWAN, I. SVIATOSLAVSKY, L. WITTENBERG, E. LOVELL, and R. ENGELSTAD, "Chamber Design for the LIBRA Light Ion Beam Fusion Reactor," Proceedings of the 8th Topical Meeting on the Technology of Fusion Energy, October 1988, Salt Lake City, UT (to be published).

6. G.L. KULCINSKI, "Technology Requirements for ICF Reactor Commercialization," Proceedings of the 8th Topical Meeting on the Technology of Fusion Energy, October 1988, Salt Lake City, UT (to be published).

7. D. BOHNE, et al., "HIBALL - A Conceptual Design Study of a Heavy-Ion Driven Inertial Confinement Fusion Power Plant," Nucl. Engr. and Design, 73, 195 (1982).

8. N.A. TAHIR and K.A. LONG, "A Study of Ignition and Burn Propagation in Reactor-Size Inertial Fusion Targets Using a Three-Temperature Plasma Simulation Model," Phys. Fluids, 30, 1820 (1987).

9. R.O. BANGERTER, "Targets for Heavy Ion Fusion," Fusion Tech., 13, 348 (1988).

10. I. SMITH, P. CORCORAN, H. NISHIMOTO, and D. WAKE, "Conceptual Design of a 30 MV Driver for LIBRA," Proc. of the Beams '88 Conference, July 1988, Karlsruhe, FRG.

11. J.J. RAMIREZ, et al., "The Four Stage Helia Experiment," Proc. of 5th IEEE Pulsed Power Conference, 1985.

12. J.J. RAMIREZ, et al., "Hermes-III, A 16 TW Short Pulse Gamma Ray Simulator," Proc. of the Beams '88 Conference, July 1988, Karlsruhe, FRG.

13. D. BIRX, et al., Proc. of 9th Conference on Appl. of Accel. in Research and Industry, Denton, TX, November 1986, to be published by Nucl. Inst. and Methods in Physics Research.

14. J.C. MARTIN, Fast Pulse Vacuum Flashover, AWRE Note SSWA, JCM/713/157, March 1971, and AFWL Dielectric Strength Note.

15. Workshop on LIBRA Diode Concept, July 1987, Albuquerque, NM.

16. J.R. FREEMAN, L. BAKER, and D.L. COOK, "Plasma Channels for Intense-Light-Ion-Beam Reactors," Nucl. Fusion, 22, 383 (1982).

17. J.J. WATROUS, G.A. MOSES, and R.R. PETERSON, "Z-PINCH -- A Multifrequency Radiative Transfer Magnetohydrodynamics Computer Code," University of Wisconsin Fusion Technology Institute Report UWFDM-584 (June 1984).

18. P.F. OTTINGER, D. MOSHER, S.A. GOLDSTEIN, "Propagation of Intense Ion Beams in Straight and Taper Z-Discharge Plasma Channels," Phys. Fluids, 23, 909 (1980).

19. G.A. MOSES, "ION -- A Code to Compute Ion Trajectories in Z-Pinch Plasma Channels," University of Wisconsin Fusion Technology Institute Report UWFDM-712 (January 1986).

20. P.F. OTTINGER, S.A. GOLDSTEIN, and D. MOSHER, "Constraints on Transportable Ion Beam Power," Naval Research Laboratory Memorandum Report 4948 (November 1982).

21. R.R. PETERSON, "WINDOW -- A Code to Compute Ion Beam Power Constraints," Fusion Power Associates Report FPA-84-6 (December 1984).

22. A.E.D. HEYLEN, "Electrical Ionization and Breakdown of Gases in a Crossed Magnetic Field," IEEE Proc., Vol. 127, Pt. A., No. 4, May 1980.

23. R.R. PETERSON, J.J. MacFARLANE, and G.A. MOSES, "CONRAD -- A Combined Hydrodynamics-Condensation/Vaporization Computer Code," UWFDM-670, University of Wisconsin Fusion Technology Institute Report (1988).

24. J.J. MacFARLANE, "IONMIX -- A Code for Computing the Equation of State and Radiative Properties of LTE and Non-LTE Plasmas," University of Wisconsin Fusion Technology Institute Report UWFDM-750, (1987), submitted to Comput. Phys. Commun.

25. J.J. MacFARLANE, R.R. PETERSON, and G.A. MOSES, "Analysis of Physical Processes in ICF Target Chambers: Application to the Laboratory Microfusion Facility," Proceedings of the 8th Topical Meeting on the Technology of Fusion Energy, October 1988, Salt Lake City, UT (to be published).

26. M. EL-AFIFY, Univ. of Wisconsin, Proceedings of the 8th Topical Meeting on the Technology of Fusion Energy, October 1988, Salt Lake City, UT (to be published).